Iraqi Journal of Physics, 2015 *Vol.13, No.26, PP. ١٢-٢٨*

Matter density distribution and longitudinal form factors for the ground and excited states of ^{17}Ne exotic nucleus

R. A. Radhi, G. N. Flaiyh, E. M. Raheem

Department of Physics, College of Science, University of Baghdad, Baghdad, Iraq

E-mail: esn_esn64@yahoo.com

Abstract

The two-frequency shell model approach is used to calculate the ground state matter density distribution and the corresponding root mean square radii of the two-proton ^{17}Ne halo nucleus with the assumption that the model space of ^{15}O core nucleus differ from the model space of extra two loosely bound valence protons. Two different size parameters b_{core} and b_{halo} of the single particle wave functions of the harmonic oscillator potential are used. The calculations are carried out for different configurations of the outer halo protons in ^{17}Ne nucleus and the structure of this halo nucleus shows that the dominant configuration when the two halo protons in the $1d_{5/2}$ orbit (^{15}O core plus two protons halo in pure $1d_{5/2}$ orbit). The calculated matter density distribution in terms of the two-frequency shell model is compared with the calculated one in terms one size parameter for all orbits to illustrate the effect of introducing one or two size parameters in calculations. The longitudinal form factors for elastic *C0* and inelastic *C2* electron scattering from ^{17}Ne nucleus are calculated for the considered configurations and for three states of each configuration which are the ground state ($J^{\pi}T = 1/2^{-}\ 3/2$) and the first two excited states ($J^{\pi}T = 3/2^{-}\ 3/2$) and ($J^{\pi}T = 5/2^{-}\ 3/2$). The electric transition strengths *B(C2)* are calculated for the excited states and for the effective nucleon charges which are used in this work and compared with the experimental values.

Key words

Matter density distribution, longitudinal form factors, exotic nuclei.

Article info.

Received: Sep. 2014
Accepted: Nov. 2014
Published: Apr. 2015

توزيع الكثافة النووية وعوامل التشكل الطولية للحالات الارضية والمتهيجة لنواة ^{17}Ne الغريبة

رعد عبدالكريم راضي، غيث نعمة فليح، احسان مشعان رحيم

قسم الفيزياء، كلية العلوم، جامعة بغداد، بغداد، العراق

الخلاصة

تم استخدام انموذج القشرة المعتمد على متذبذبين توافقيين في حساب توزيع الكثافة النووية في الحالة الارضية وانصاف الاقطار المقابلة لها لنواة الهالة ^{17}Ne وعلى فرض ان فضاء نواة القلب ^{15}O يختلف عن فضاء البروتونين خارج هذا القلب. تم استخدام قيمتين مختلفتين للثابت التوافقي للدوال الموجية لجهد المتذبذب التوافقي هما b_{core} الخاص بالقلب والاخر b_{halo} الخاص بالهالة. اجريت الحسابات لعدة ترتيبات للبروتونين الهالة خارج القلب ومن خلال تفسير النتائج وجد بأن الترتيب السائد يتمثل بكون البروتونين الهالة في المدار $1d_{5/2}$ بمعنى (نواة القلب ^{15}O مضاف اليها بروتونين هالة في المدار $1d_{5/2}$). تم مقارنة توزيع الكثافة النووية المحسوب بدلالة انموذج القشرة المعتمد على متذبذبين توافقيين مع التوزيع المحسوب بدلالة ثابت توافقي واحد لجميع المدارات وذلك لتوضيح تأثير ادخال ثابت توافقي واحد أو اثنين في الحسابات. تم ايضا حساب عوامل التشكل الطولية للاستطارة الالكترونية المرنة (*C0*) وغير المرنة (*C2*) للنواة ^{17}Ne للترتيبات المدروسة ولثلاثة حالات لكل ترتيب وهي الحالة الارضية ($J^{\pi}T = 1/2^{-}\ 3/2$) والحالتين المتهيجتين ($J^{\pi}T = 3/2^{-}\ 3/2$) و($J^{\pi}T = 1/2^{-}\ 3/2$). كما وتم حساب شدة الانتقال الكهربائي المختزل *B(C2)* للحالات المتهيجة ولجميع الشحنات الفعالة المستخدمة في موضوع البحث وتم مقارنتها مع النتائج العملية.

Introduction

The progress of the new generation of experimental facilities on radioactive ion beams opens the opportunity to investigate unknown regions of exotic nuclei, far from the beta stability line, where these nuclei having a large asymmetry in the proton-to-neutron ratio. With access to exotic nuclei at the very limits of nuclear stability, the physics of the neutron and proton driplines has become the focus of interest. The driplines are the limits of the nuclear landscape, where additional protons or neutrons can no longer be kept in the nucleus and they literally drip out [1].

The field of halo nuclei has generated much excitement and many hundreds of papers since its discovery in the mid-1980's. While early β- and γ-decay studies of many of these nuclei yielded information about their lifetimes and certain features of their structure, credit for their discovery should go mostly to Tanihata [2,3] for the work of his group at Lawrence Berkeley Laboratory's Bevalac in 1985 on the measurement of the very large interaction cross sections of certain neutron-rich isotopes of helium and lithium, along with Hansen and Jonson for their pioneering paper two years later in which the term 'halo' was first applied to these nuclei [4]. Halo nuclei are very weakly-bound exotic states of nuclear matter in which the outer one or two valence nucleons (usually neutrons) are spatially decoupled from a relatively tightly bound core such that they spend more than half their time beyond the range of the binding nuclear potential. In this sense, the halo is a threshold phenomenon in which the 'halo' nucleons quantum tunnel out to large distances, giving rise to extended wave function tails and hence large overall matter radii. The halo nucleons tend to be in low relative orbital angular momentum states so as not to be confined by the centrifugal barrier.

In the proton-rich or neutron-rich nuclei, a few exotic features have been observed. These includes a large extension of mass density distribution, referred to as halo or skin structure [2], a narrow momentum distribution [5] and a large concentration of the dipole strength distribution at low energies [6–8]. There are two main classes of halo state; the two-body halos with one nucleon surrounding the core, like the one-neutron halos ^{11}Be and ^{19}C and the one-proton halo ^{8}B and the Borromean three-body halos with two valence nucleons around the core like ^{6}He, ^{11}Li and ^{14}Be. The so called Borromean structure has also been discussed extensively [9,10]. The Borromean is defined as a three-body bound system in which any two-body subsystem does not bound. The pairing interaction between the valence neutrons plays an essential role in stabilizing these nuclei [9].

The extraction of the nucleon density distribution and nuclear radius from experimental total reaction cross section of nucleus-nucleus collisions has been carried out almost exclusively by using the Glauber model in the optical-limit approximation. The first series of measurements of interaction cross-sections using radioactive beams was performed by Tanihata and coworkers in 1985 [2,3]. The σ_I were measured with transmission-type experiments. Their classical results for He and Li isotopes were one of the main experimental hints of the existence of halo states in nuclei. The measured interaction cross sections were used to extract root mean square radii (rms) using Glauber-model analysis. The standard shell model fails to describe many of the essential features of halo nuclei (although it has proved to be of importance in providing spectroscopic information on a number of exotic nuclei) and many theorists

acknowledge that there is a real need to go beyond the conventional shell model [12].

The two-frequency shell-model approach (TFSM) was employed successfully on halo nuclei [13,14], for both valence energy and rms radii. Within this model, one uses harmonic-oscillator (HO) wave functions with two oscillator size parameters, b_{core} and b_{halo} for the core and halo orbits, respectively. This technique will enable one to work freely on each part by changing $b_{core(halo)}$ till one can get a fit with some experimental results.

In the present work, the two proton halo structure of ^{17}Ne is studied with the assumption that the two valence protons forming the halo. Shell- model configuration mixing is carried out by using a model space for the ^{15}O core nucleus different from that of the two halo protons where the spatial space of the valence protons is much larger than the core. The elastic electron scattering form factor, matter density distribution of the ground state ($J^{\pi} = 1/2^{-}$) and the inelastic electron scattering form factors of the two excited states ($J^{\pi} = \frac{3}{2}^{-}, \frac{5}{2}^{-}$) of the exotic ^{17}Ne nucleus are calculated.

Theory

The longitudinal (Coulomb) one-body operator for a nucleus with multipolarity J and momentum transfer q is given by [15]:

$$\hat{T}_{JM}(q) = \int d\vec{r} j_J(qr) Y_{JM}(\Omega) \hat{\rho}(\vec{r}) \quad (1)$$

where $j_J(qr)$ is the spherical Bessel's function, $Y_{JM}(\Omega)$ is the spherical harmonics and $\hat{\rho}(\vec{r})$ is the density operator, which is given by:

$$\rho(\vec{r}) = \sum_k e(k) \delta(\vec{r} - \vec{r}_k) \quad (2)$$

The longitudinal (Coulomb) one-body operator becomes:

$$\hat{T}_{JM}(q, \vec{r}) = \sum_{k=1}^{n} e(k) j_J(qr)_k Y_{JM}(\Omega_k) \quad (3)$$

where $e(k)$ is the electric charge for the k-th nucleon. Since $e(k) = 0$ for neutron, there should appear no direct contribution from neutrons; however, this point requires further attention: The addition of a valence neutron will induce polarization of the core into configurations outside the adopted model space. Such core polarization effect is included through perturbation theory which gives effective charges for the proton and neutron. Eq. (3) can be written as:

$$\hat{T}_{JM}(q, \vec{r}) = \sum_{k=1}^{n} \left(e_{\mathrm{p}} \frac{1 + \tau_z(k)}{2} + e_{\mathrm{n}} \frac{1 - \tau_z(k)}{2} \right) j_J(qr)_k Y_{JM}(\Omega_k) \quad (4)$$

where $\tau_z|\mathrm{p}\rangle = |\mathrm{p}\rangle$ and $\tau_z|\mathrm{n}\rangle = -|\mathrm{n}\rangle$. Eq. (4) can be rearranged to

$$\hat{T}_{JM}(q, \vec{r}) = \sum_{k=1}^{n} \left(\frac{e_{\mathrm{p}} + e_{\mathrm{n}}}{2} + \frac{e_{\mathrm{p}} - e_{\mathrm{n}}}{2} \tau_z(k) \right) j_J(qr)_k Y_{JM}(\Omega_k) \quad (5)$$

which can be written as:

$$\hat{T}_{JM}(q, \vec{r}) = e_{\mathrm{IS}} \sum_{k=1}^{n} j_j(qr)_k Y_{JM}(\Omega_k) + e_{\mathrm{IV}} \sum_{k=1}^{n} j_j(qr)_k Y_{JM}(\Omega_k) \tau_z(k) \quad (6)$$

where $e_{\rm IS}=\dfrac{e_{\rm p}+e_{\rm n}}{2}$ and $e_{\rm IV}=\dfrac{e_{\rm p}-e_{\rm n}}{2}$ (7)

are the isoscalar and isovector charges, respectively. The bare proton and neutron charges are denoted by $e_{\rm p}$ and $e_{\rm n}$, respectively.

The reduced matrix element in both spin-isospin spaces of the longitudinal operator $\hat{T}_\Lambda$ is expressed as the sum of the product of the elements of the one-body density matrix (OBDM) $X^{\Lambda}_{\Gamma_f\Gamma_i}(\alpha,\beta)$ times the single-particle matrix elements, and is given by [16]:

$$\left\langle \Gamma_f \|\|\tilde{\hat{T}}_\Lambda\|\|\Gamma_i\right\rangle=\sum_{\alpha\beta}X^{\Lambda}_{\Gamma_f\Gamma_i}(\alpha,\beta)\left\langle\alpha\|\|\tilde{\hat{T}}_\Lambda\|\|\beta\right\rangle \quad (8)$$

where α and β label single-particle states (isospin is included) for the shell model space. The states $|\Gamma_i\rangle$ and $|\Gamma_f\rangle$ are described by the model space wave functions. Greek symbols are used to denote quantum numbers in coordinate space and isospace, i.e $\Gamma_i\equiv J_iT_i$, $\Gamma_f\equiv J_fT_f$ and $\Lambda\equiv JT$.

The role of the core and the truncated space can be taken into consideration through a microscopic theory, which combines shell model wave functions and configurations with higher energy as first order perturbation to describe *EJ* excitations: these are called core polarization effects. The reduced matrix elements of the electron scattering operator $\hat{O}_\Lambda$ is expressed as a sum of the model space (MS) contribution and the core polarization (CP) contribution, as follows:

$$\left\langle \Gamma_f \|\|\tilde{\hat{T}}_\Lambda\|\|\Gamma_i\right\rangle=\left\langle \Gamma_f \|\|\hat{T}_\Lambda\|\|\Gamma_i\right\rangle_{\rm MS}+\left\langle \Gamma_f \|\|\Delta\hat{T}_\Lambda\|\|\Gamma_i\right\rangle_{\rm CP} \quad (9)$$

which can be written as:

$$\left\langle \Gamma_f \|\|\tilde{\hat{T}}_\Lambda\|\|\Gamma_i\right\rangle=\sum_{\alpha\beta}X^{\Lambda}_{\Gamma_f\Gamma_i}(\alpha,\beta)\left[\left\langle\alpha\|\|\hat{T}_\Lambda\|\|\beta\right\rangle+\left\langle\alpha\|\|\Delta\hat{T}_\Lambda\|\|\beta\right\rangle\right] \quad (10)$$

According to the first-order perturbation theory, the single particle core-polarization term is given by [17]:

$$\left\langle\alpha\|\|\Delta\tilde{\hat{T}}_\Lambda\|\|\beta\right\rangle=\left\langle\alpha\|\|\hat{T}_\Lambda\frac{Q}{E_i-H_0}\mathrm{V}_{res}\|\|\beta\right\rangle+\left\langle\alpha\|\|\mathrm{V}_{res}\frac{Q}{E_f-H_0}\hat{T}_\Lambda\|\|\beta\right\rangle \quad (11)$$

where the operator Q is the projection operator onto the space outside the model space. The single particle core-polarization terms given in Eq. (11) are written as [17]:

$$\left\langle\alpha\|\|\Delta\hat{T}_\Lambda\|\|\beta\right\rangle=$$

$$\sum_{\alpha_1\alpha_2\Gamma}\frac{(-1)^{\beta+\alpha_2+\Gamma}}{\varepsilon_\beta-\varepsilon_\alpha-\varepsilon_{\alpha_1}+\varepsilon_{\alpha_2}}(2\Gamma+1)\begin{Bmatrix}\alpha & \beta & \Lambda\\ \alpha_2 & \alpha_1 & \Gamma\end{Bmatrix}\sqrt{(1+\delta_{\alpha_1\alpha})(1+\delta_{\alpha_2\beta})}$$

$$\times\left\langle\alpha\alpha_1|\,\mathrm{V}_{res}\,|\beta\alpha_2\right\rangle_\Gamma\left\langle\alpha_2\|\|\hat{T}_\Lambda\|\|\alpha_1\right\rangle$$

+ terms with α_1 and α_2 exchanged with an overall minus sign (12)

where the index α_1 runs over particle states and α_2 over hole states and ε is the single-particle energy, and is calculated according to [17]:

$$\varepsilon_{n\ell j}=(2n+\ell-1/2)\hbar\omega+\begin{cases}-\dfrac{1}{2}(\ell+1)\langle f(r)\rangle_{n\ell} & \text{for} j=\ell-1/2\\ \dfrac{1}{2}\ell\langle f(r)\rangle_{n\ell} & \text{for} j=\ell+1/2\end{cases} \quad (13)$$

with $\langle f(r)\rangle_{n\ell}\approx -20\,A^{-2/3}$

and $\hbar\omega=45\,A^{-1/3}-25\,A^{-2/3}$

Higher energy configurations are taken into consideration through 1p-1h $n\hbar\omega$ excitations. For the residual two-body interaction V_{res}, the M3Y interaction of Bertsch *et al*. [18] is adopted. The form of the potential is defined in Eqs. (1)-(3) in Ref. [18]. The parameters of 'Elliot' are used which are given in Table 1 of the mentioned reference. A transformation between *LS* and *jj* is used to get the relation between the two-body shell model matrix elements and the relative and center of mass coordinates, using the harmonic oscillator radial wave functions with Talmi-Moshinsky transformation [19, 20].

Using Wigner-Eckart theorem, the single particle matrix elements reduced in both spin and isospin, are written in terms of the single-particle matrix elements reduced in spin only:

$$\left\langle \alpha_2 \| \hat{T}_\Lambda \| \alpha_1 \right\rangle = \sqrt{\frac{2T+1}{2}} \sum_{t_z} I_T(t_z) \left\langle j_2 \| \hat{T}_{jt_z} \| j_1 \right\rangle \quad (14)$$

with:

$$I_T(t_z) = \begin{cases} 1 & \text{for} \quad T = 0 \\ (-1)^{1/2 - t_z} & \text{for} \quad T = 1 \end{cases} \quad (15)$$

where t_z= 1/2 for a proton and -1/2 for a neutron. The single particle matrix element of the electric transition operator reduced in spin space is:

$$\left\langle j_2 \| \hat{T}_{Jt_z} \| j_1 \right\rangle = e_{t_z} \left\langle j_2 \| Y_J \| j_1 \right\rangle \left\langle n_2 \ell_2 | j_J(qr) | n_1 \ell_1 \right\rangle \quad (16)$$

where $|n\ell\rangle$ is the single-particle radial wave function.

The reduced single-particle matrix element of the longitudinal operator becomes:

$$\left\langle \alpha_2 \| \hat{T}_\Lambda \| \alpha_1 \right\rangle = e_T \sqrt{2(2T+1)} \left\langle j_2 \| Y_J \| j_1 \right\rangle \left\langle n_2 \ell_2 | j_J(qr) | n_1 \ell_1 \right\rangle \quad (17)$$

where e_T is the isoscalar (T = 0) and isovector (T = 1) charges.

Electron scattering form factor involving angular momentum J and momentum transfer q, between initial and final nuclear shell model states of spin $J_{i,f}$ and isospin $T_{i,f}$ are [21]:

$$|F_J(q)|^2 = \frac{4\pi}{Z^2(2J_i+1)} \left| \sum_{T=0,1} (-1)^{T_i - T_z} \begin{pmatrix} T_f & T & T_i \\ -T_z & 0 & T_z \end{pmatrix} \left\langle J_f T_f \| \tilde{\hat{T}}_{JT} \| J_i T_i \right\rangle \right|^2 F_{cm}^2(q) F_{fs}^2(q) \quad (18)$$

where $F_{cm}(q)$ is the center of mass correction which is given by $F_{cm}(q) = e^{-q^2 b^2 / 4A}$, with b is the harmonic oscillator size parameter and $F_{fs}(q)$ is the finite size correction given by $F_{fs}(q) = \left[1 + (q/4.33 fm^{-1})^2\right]^{-2}$ [22].

The reduced electromagnetic transition probability $B(CJ\uparrow)$ can be obtained from the longitudinal form factor evaluated at $q = k = \frac{E_x}{\hbar c}$ (photon point) as [23]:

$$B(CJ\uparrow) = \frac{Z^2}{4\pi} \left[\frac{(2J+1)!!}{k^J} \right]^2 |F_J(k)|^2 \quad (19)$$

The relation between the $B(CJ)$ values for the emission ↓ and absorption ↑ process is [17]:

$$B(CJ\downarrow) = \frac{2J_i + 1}{2J_f + 1} B(CJ\uparrow) \quad (20)$$

where i and f are the initial and final states, respectively.

For electromagnetic transition, the $B(EJ)$ value can be calculated directly in terms of the electric multipole transition operator [17]:

$$\hat{O}_{JM}(\vec{r}) = \sum_{k=1}^{n} e(k) r_k^J Y_{JM}(\Omega_k)$$

so, replacing the operator T in all the above equations by the operator O, Eq.(17) for the reduced single particle matrix element becomes:

$$\left\langle \alpha_2 \| \hat{O}_\Lambda \| \alpha_1 \right\rangle = e_T \sqrt{2(2T+1)} \left\langle j_2 \| Y_J \| j_1 \right\rangle \left\langle n_2 \ell_2 | r^J | n_1 \ell_1 \right\rangle \quad (21)$$

The reduced electromagnetic transition probability $B(EJ)$ is defined as [17]:

$$B(EJ)=\frac{1}{(2J_i+1)}\left|\sum_{T=0,1}(-1)^{T_i-T_z}\begin{pmatrix} T_f & T & T_i \\ -T_z & 0 & T_z\end{pmatrix}\left\langle J_fT_f\|\|\tilde{\hat{O}}_{JT}\|\|J_iT_i\right\rangle\right|^2$$

which can be written as:

$$B(EJ)=\frac{1}{(2J_i+1)}\left|\sum_{T=0,1}e_T(-1)^{T_i-T_z}\begin{pmatrix} T_f & T & T_i \\ -T_z & 0 & T_z\end{pmatrix}\left\langle J_fT_f\|\|\tilde{\hat{M}}_{JT}\|\|J_iT_i\right\rangle\right|^2 \quad (22)$$

where $\tilde{M}_{JT}=\left\langle J_fT_f\|\|\tilde{\hat{M}}_{JT}\|\|J_iT_i\right\rangle$. The isoscalar ($T$=0) and isovector ($T$=1) charges are given by $e_0=e_{\rm IS}=\frac{1}{2}e, \quad e_1=e_{\rm IV}=\frac{1}{2}e.$

The reduced electromagnetic transition probability can be represented in terms of only the model space matrix elements, but with effective charges, as:

$$B(EJ)=\frac{1}{(2J_i+1)}\left|\sum_{T=0,1}e_T^{eff}(-1)^{T_i-T_z}\begin{pmatrix} T_f & T & T_i \\ -T_z & 0 & T_z\end{pmatrix}\left\langle J_fT_f\|\|\hat{M}_{JT}\|\|J_iT_i\right\rangle\right|^2 \quad (23)$$

Then the isoscalar and isovector effective charges are given by:

$$e_T^{\rm eff}=\frac{M_{JT}+\Delta M_{JT}}{2M_{JT}}e=\frac{e_p^{\rm eff}+(-1)^T e_n^{\rm eff}}{2} \quad (24)$$

The proton and neutron effective charges can be obtained as follows:

$e_{\rm p}^{\rm eff}=e_0^{\rm eff}+e_1^{\rm eff}$ and $e_n^{\rm eff}=e_0^{\rm eff}-e_1^{\rm eff}$

The above effective charges work for mixed isoscalar and isovector transitions. For pure isoscalar transition; the polarization charge δe is given by:

$$\delta e=\frac{\Delta M_J}{2M_J}e \quad (25)$$

and the effective charges for the proton and neutron becomes

$$e_{\rm p}^{\rm eff}=e+\delta e, \quad e_{\rm n}^{\rm eff}=\delta e \quad (26)$$

The longitudinal form factor, $F_J(q)$ can be written as:

$$F_J(q)=\frac{4\pi}{N_{t_Z}}=\int_0^\infty dr\, r^2\, j_J(qr)\,\rho_{J,t_Z}(r) \quad (27)$$

where the normalization factor N_{t_Z} is defined as:

$$N_{t_Z}=\left\{\begin{matrix} A\,(mass\ \ number\ ) \\ Z\,(proton\ \ number\ ) \\ N\,(neutron\ \ \ number\ )\end{matrix}\right\}$$

From Eqs. (18) and (27), the nucleon transition density can be found to be [16]:

$$\rho_{J,t_Z}(r)=\frac{1}{4\pi}\sqrt{\frac{4\pi}{2J_i+1}}\sum_{a,b}OBDM\,(J_i,J_f,a,b,J,t_Z)$$

$$\times\left\langle n_a\tfrac{1}{2}j_a\|Y_J(\Omega_r)\|n_b\tfrac{1}{2}j_b\right\rangle R_{n_al_{n_a}}(r)\,R_{n_bl_{n_b}}(r) \quad (28)$$

the corresponding mean square radius is given in terms of the nucleon density as [24]:

$$\left\langle r^2\right\rangle=\frac{4\pi}{A}\int_0^\infty\rho(r)\,r^4\,dr \quad (29)$$

or it is given in terms of the occupation number as :

$$\left\langle r^2\right\rangle=\frac{1}{A}\sum_{a,t_Z}n_a,t_Z(t_Z,j_a)(2n_a+l_a-\frac{1}{2})b^2 \quad (30)$$

where $n_a,t_Z(t_Z,j_a)$ is the average occupation number in each orbit.

As halo nuclei are consist of a compact core plus a number of outer nucleons loosely bound and spatially extended far from the core, it is suitable to separate the density distribution of Eq. (28) into two parts. The first is connected to the core nucleons while the second is connected to the halo nucleons, so the matter density of the whole halo nucleus becomes:

$$\rho_m(r)=\rho^{core}(r)+\rho^{halo}(r) \quad (31)$$

Results and discussion

The lightest bound isotope of neon is ^{17}Ne and its two outer protons separation energy is S_{2p}= 950 keV. The Borromean character of ^{17}Ne combined with its low two-proton separation energy makes it an obvious candidate to be a two-proton halo nucleus [25,26]. The proton drip line ^{17}Ne ($J^{\pi}T = 1/2^{-}\ 3/2$; half life $t_{1/2}$=109.2 ms) [27] has halo structure, which coupled a ^{15}O core ($J^{\pi}T = 1/2^{-}\ 1/2$; half life $t_{1/2}$=122.24 s) [27] and outer two protons assumed to be in sd model space (2s-1d orbits) or a pure $1d_{5/2}$, a pure $1d_{3/2}$, a pure $2s_{1/2}$. The two-frequency shell model (TFSM) approach [13,14] is employed to calculate the ground state matter density distributions, elastic, inelastic electron scattering form factors and the reduced transition probabilities *B(C2)* for ^{17}Ne nucleus with different model spaces for the core and the extra two halo protons. The single particle harmonic oscillator wave functions are used with two different oscillator size parameters b_{core} for the core orbits and b_{halo} for the two halo protons orbit. The one-body density matrix elements OBDM values for all considered configurations in the present work are obtained by the shell model calculations that performed via the computer code OXBASH [28] using the PSD model space with Millener-Kurath (MK) [29] effective interaction.

Ground state

$J^{\pi}T$: $1/2^{-}\ 3/2$ (0.0 MeV) state

The size parameters of the core and the outer two halo protons are chosen to reproduce the rms matter radius which is consisting with the measured value. b_{core} is fixed at 1.633 fm, this value gives the rms matter radius of ^{15}O core nucleus equal to 2.44 fm, which is consisting with the measured value 2.44 ± 0.04 fm [11]. The size parameter for the outer two protons halo b_{halo} is chosen to be 2.368 fm to reproduce the rms matter radius of ^{17}Ne nucleus 2.75 fm that is consisting with the measured value 2.75 ± 0.07 fm [11]. The proton and neutron rms of the ^{17}Ne nucleus are calculated as rms_p=2.954 fm and rms_n=2.430 fm and the difference between these values is 0.524 fm means that the ^{17}Ne nucleus has a halo structure.

The ground state matter density distributions $\rho_m(r)$ in (fm^{-3}) for ^{17}Ne nucleus are calculated and plotted in Fig.(1) as a function of nuclear radius r in (fm). The plus symbols are the calculated matter density of ^{15}O core plus two protons with the assumption that the outer two protons move in the sd model space. The dash-dotted, dashed and solid curves are the calculated matter density of ^{15}O core plus two protons when the outer two protons move in the pure $2s_{1/2}$, pure $1d_{3/2}$ and pure $1d_{5/2}$ orbits, respectively. The filled circles are the experimental matter density deduced from the Glauber model using the fitting procedure with (HO+HO) density function [30]. The poor agreement in Fig.1(a) between all calculated ground state matter density distributions with (b_{core}=1.633 fm and b_{halo}=2.368 fm), and the fitted data motivate us to recalculate the size parameters and the corresponding rms values of the core and the outer two halo protons, where b_{core} is fixed at 1.606 fm and b_{halo} is fixed at 2.640 fm. These values gives rms matter radius of ^{15}O core nucleus equal to 2.40 fm and rms of ^{17}Ne nucleus equal to 2.82 fm which are consisting with the measured values 2.44 ± 0.04 fm and 2.75 ± 0.07 fm, respectively. The proton and neutron rms are calculated as rms_p=3.086 fm and rms_n=2.390 fm and rms_p-rms_n=0.696 fm.

Fig.1(b) shows the calculated ground state matter density distributions for all considered configurations of ^{17}Ne with (b_{core}=1.606 fm and b_{halo}=2.640 fm), and the

fitted data. It is evident that the solid curve describes the fitted data in most of the *q* values more than the other curves, and we can say that the dominant configuration of the ^{17}Ne nucleus is (^{15}O core plus two protons halo in pure $1d_{5/2}$ orbit) with occupation numbers $(1s_{1/2})^4$, $(1p_{3/2})^{7.9144}$, $(1p_{1/2})^{3.0856}$ and $(1d_{5/2})^2$. The calculations showed a long tail in the density distribution, which is interpreted as evidence for the two valence protons halo.

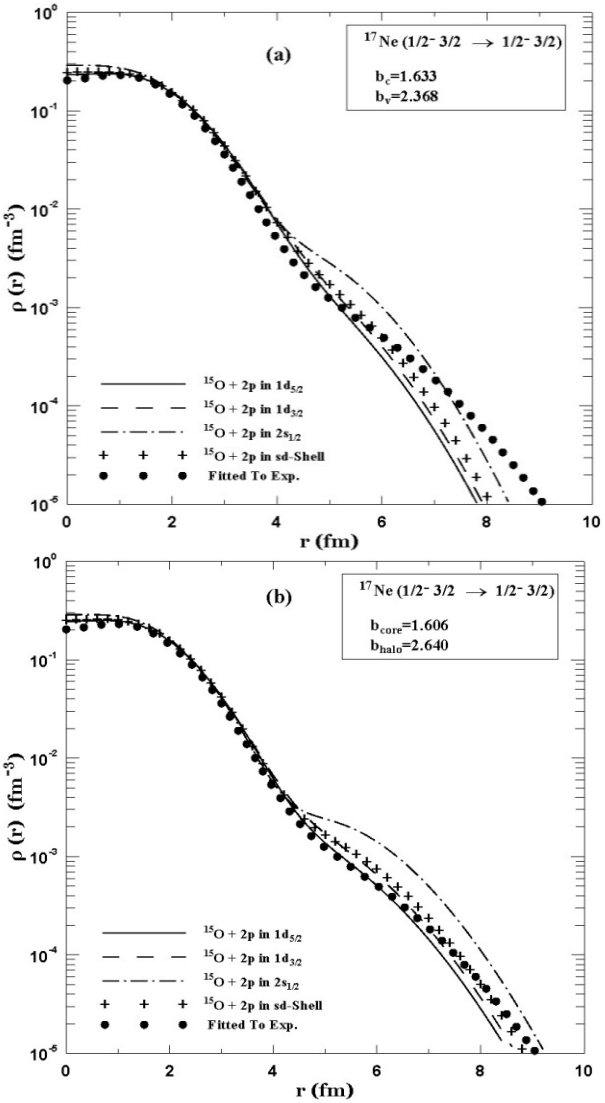

Fig. 1: The calculated ground state matter densities of ^{17}Ne nucleus. the filled circles are the experimental data extracted from Glauber model [30].

Fig. 2, shows a comparison between the calculated ground state matter density distribution of ^{17}Ne with ^{15}O core-two protons in $1d_{5/2}$ (TFSM; solid curve, b_{core}=1.606 fm, b_{halo}=2.640 fm), the calculated ground state matter density distribution of ^{17}Ne with ^{15}O core-two protons in $1d_{5/2}$ (TFSM; dashed curve, b_{core}=1.633 fm, b_{halo}=2.368 fm), the calculated ground state matter density distribution with only one size parameter for all orbits (one size parameter ; dotted curve, b=1.827 fm) and the fitted data (filled circles). The poor agreement between dotted curve and fitted data especially at the long tail region of the fitted data is due to carry out the calculations by taking the whole model space of ^{17}Ne nucleons as a one part (one harmonic oscillator size parameter) where it must dividing into two parts one for core nucleons and the other for extra two halo protons to get a coincidence with the fitted data as in the dashed and solid curves where the solid curve is markedly interpreting the long tail behavior because of using a suitable values of the size parameters.

The longitudinal form factors *C0* for elastic electron scattering from ^{17}Ne nucleus are calculated for three configurations which are ^{15}O core plus two protons in (sd-shell, $1d_{3/2}$ orbit and $1d_{5/2}$ orbit). Appropriate oscillator size parameters which used are either (b_{core}=1.633 fm and b_{halo}=2.368 fm) or (b_{core}=1.606 fm and b_{halo}=2.640 fm) to get a good agreement between the calculations (solid curves) and the experimental data of ^{20}Ne nucleus (open circles) as shown in Figs. (3-5).

Since ^{17}Ne halo nucleus is unstable (short-lived), the calculated longitudinal elastic form factors *C0* are compared with the experimental one for ^{20}Ne (stable isotope) which is taken from Refs. [31,32]. In spite of the nucleons in ^{20}Ne nucleus are more than these in ^{17}Ne nucleus, the

significant difference between the *C0* form factors of the ^{17}Ne halo nucleus and that of stable ^{20}Ne nucleus is mainly attributed to the harmonic oscillator size parameters of both nuclei, which is in ^{17}Ne nucleus bigger than that in ^{20}Ne nucleus. According to this bases, we can concludes that the differences between the calculated *C0* form factors of ^{17}Ne and experimental data of ^{20}Ne nucleus are attributed to the last two protons in the two nuclei.

It is so apparent from the Figs. (3-5) that there is a reasonable interpretation of the experimental results by the calculations.

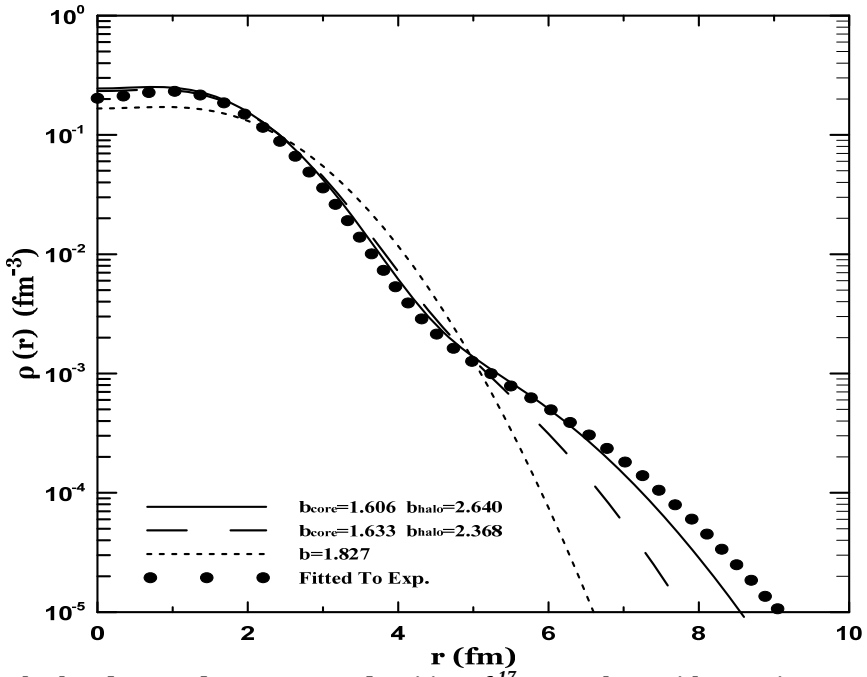

Fig. 2: The calculated ground state matter densities of ^{17}Ne nucleus with one size parameter value (dotted curve) and with ^{15}O core-two protons in $1d_{5/2}$ orbit (dashed and solid curves, respectively). The filled circles are the experimental data extracted from Glauber model [30].

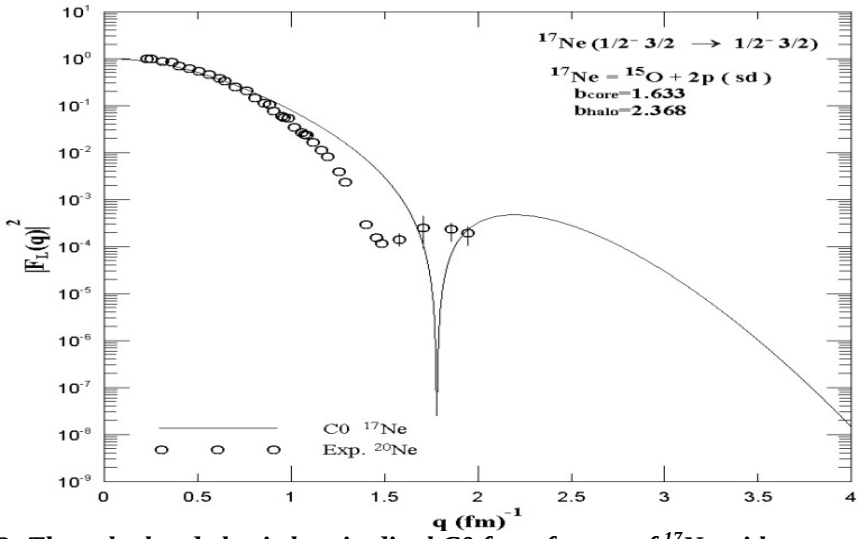

Fig. 3: The calculated elastic longitudinal C0 form factors of ^{17}Ne with two protons in sd-shell. the experimental data are taken from Refs [31,32].

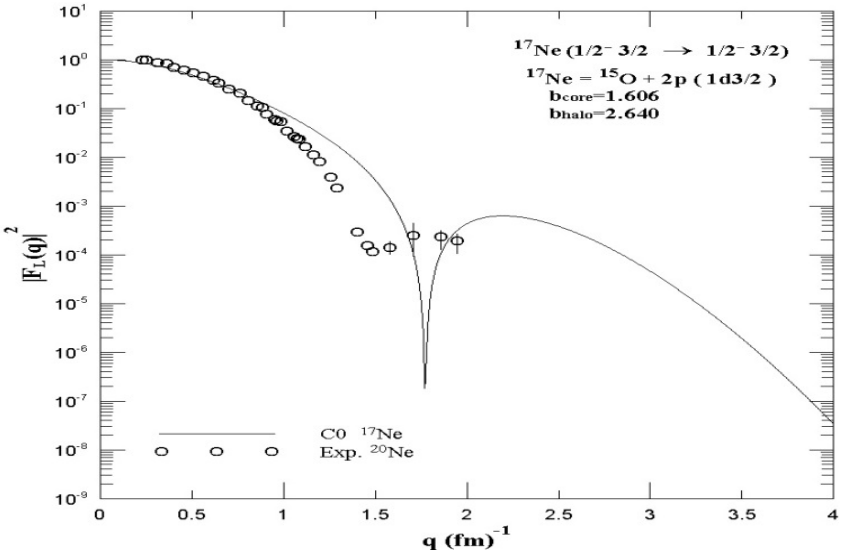

Fig. 4: The calculated elastic longitudinal C0 form factors of ^{17}Ne with two protons in $1d_{3/2}$ orbit. the experimental data are taken from Refs [31,32].

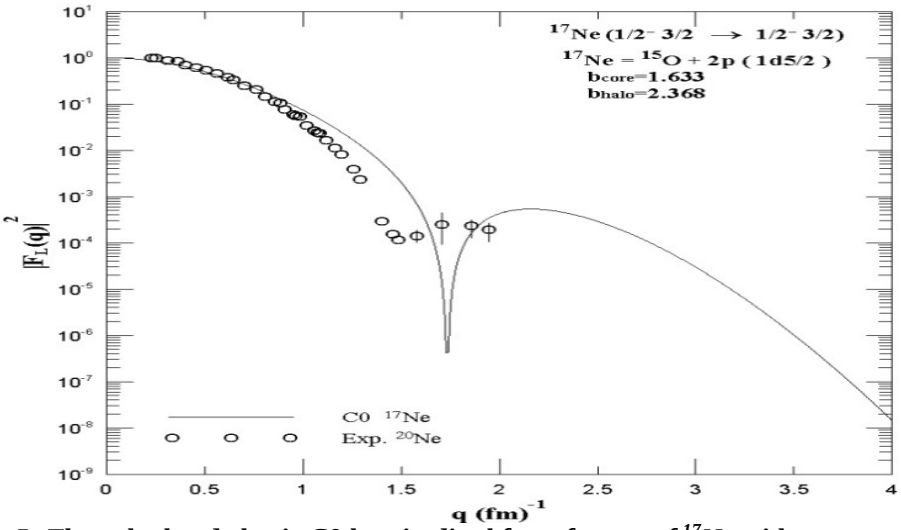

Fig. 5: The calculated elastic C0 longitudinal form factors of ^{17}Ne with two protons in $1d_{5/2}$ orbit. the experimental data are taken from Refs [31,32].

Excited States

The *C2* coulomb form factors of the inelastic electron scattering from ^{17}Ne nucleus are calculated for three configurations: ^{15}O core plus two protons in (sd-shell, pure $1d_{3/2}$ orbit and pure $1d_{5/2}$ orbit). The calculations are executed for the first two excited states of each configuration which are:

$(J^{\pi}T = 3/2^{-}\,3/2)$ and $(J^{\pi}T = 5/2^{-}\,3/2)$

$J^{\pi}T : 3/2^{-}\,3/2$ state

In this transition, the nucleus is excited from the ground to state $(J^{\pi}T = 1/2^{-}\,3/2)$ to the state $(J^{\pi}T = 3/2^{-}\,3/2)$. The experimental reduced transition probability *B(C2↑)* value of this transition is equal to $66^{+18}_{-25}\,e^2\,fm^4$ [33].

We first consider the two halo protons of ^{17}Ne nucleus are distributed over sd-shell orbits. The excitation energy of this state is of 2.104 MeV. The harmonic oscillator size parameters that used in calculations are b_{core}=1.633 fm and b_{halo}=2.368 fm, where these values are calculated in terms of the experimental rms when ^{17}Ne nucleus in its ground state. In Fig.(6), the theoretical calculations of the *C2* Coulomb form factors are presented. Four theoretical curves are shown: Dotted curve displays the calculations in terms of the bare nucleon charges (e_p=1.0 e , e_n=0.0 e), dash-dotted and dashed curves are the calculations in terms of effective charges that chosen to account for the core polarization effects (e_p=1.033 e, e_n=0.033 e) and (e_p=1.3 e, e_n=0.3 e), respectively; while the solid curve shows the result with standard nucleon charges (e_p=1.3 e, e_n=0.5 e). It is apparent from Fig. 6, that all calculated *C2* form factors are approximately coinciding with each other within the momentum transfer range q =0 - 2.3 fm^{-1}. The calculated *C2* with bare charges (dotted curve) have only one diffraction minimum located at q =1.36 fm^{-1}, whereas those calculated with standard and effective charges have two diffraction minima. The theoretical and experimental results of the reduced transition probability $B(C2\uparrow)$ are given in Table 1. It is so clear from the table that the calculations with all used nucleon charges overestimates the experimental value (excessively large).

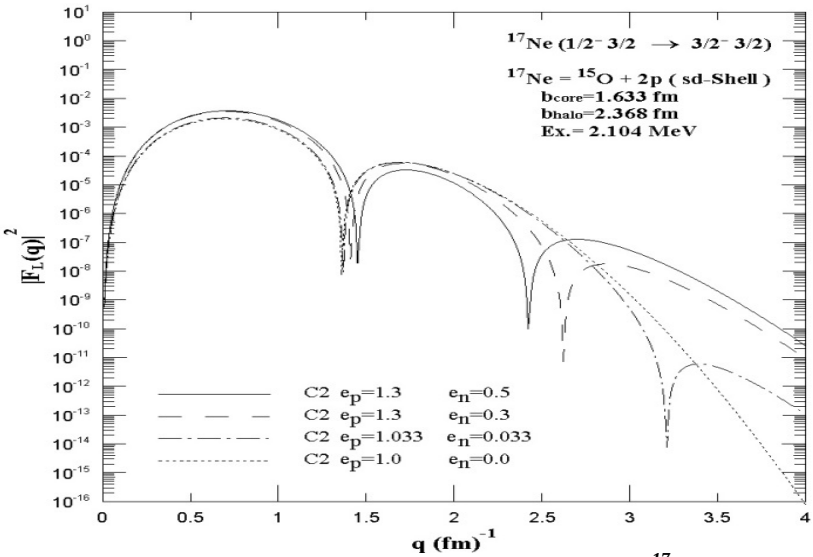

Fig. 6: The calculated inelastic longitudinal C2 form factors of ^{17}Ne with two protons in sd-shell and for ($J^{\pi}T = 3/2^{-}\,3/2$) state.

The second configuration of the two halo protons suppose that these protons are in a pure $1d_{3/2}$. The excitation energy of these protons is 2.260 MeV. The harmonic oscillator size parameters that used in the calculations are b_{core}=1.606 fm and b_{halo}=2.640 fm, where these values lead to a significant improvement in the calculated ground state nucleon density distributions.

The longitudinal *C2* electron scattering form factors are shown in Fig. 7, where three values of the nucleon charges are used and each value gives a specific curve. Dotted curve displays the calculations in terms of the bare nucleon charges (e_p=1.0 e, e_n=0.0e), dashed curve reflect the calculations by using the core polarization effective charges (e_p=1.111 e, e_n=0.265 e) and solid curve

refers to using standard nucleon charges (e_p=1.3 e , e_n=0.5 e). All curves are deviate from each other beyond $q \approx 1.25$ fm^{-1}, and there is one diffraction minimum associated with dotted and solid curves while dashed curve gives two diffraction minima. The agreement between the calculated and the experimental transition strengths $B(C2\uparrow)$ is remarkably good especially with using bare and effective nucleon charges, as that shown in Table 1.

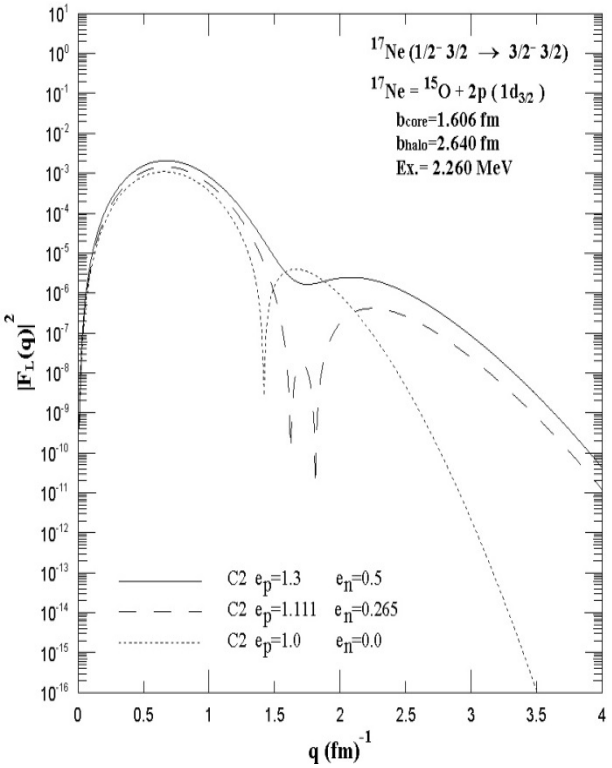

Fig. 7: The calculated inelastic longitudinal C2 form factors of ^{17}Ne with two protons in 1d$_{3/2}$ orbit and for ($J^\pi T = 3/2^- 3/2$) state.

The third configuration assumes that the two halo protons are in a pure $1d_{5/2}$ orbit. The size parameters are taken to be b_{core}=1.633 fm and b_{halo}=2.368 fm. The calculations for the *C2* transition from the ground state ($J^\pi T = 1/2^- 3/2$) to the ($J^\pi T = 3/2^- 3/2$) state at excitation energy of 0.955 MeV are shown in Fig. 8. Three theoretical curves are shown: Dotted, dashed and solid curves correspond to the calculations with using bare, effective and standard nucleon charges respectively. Two diffraction minima are exhibited by dashed curve, besides there is one diffraction minimum given by dotted and solid curves. As shown from Table 1, there is a remarkable agreement between experimental value of the transition strength $B(C2\uparrow)$ and those of calculated values especially at using bare and effective nucleon charges.

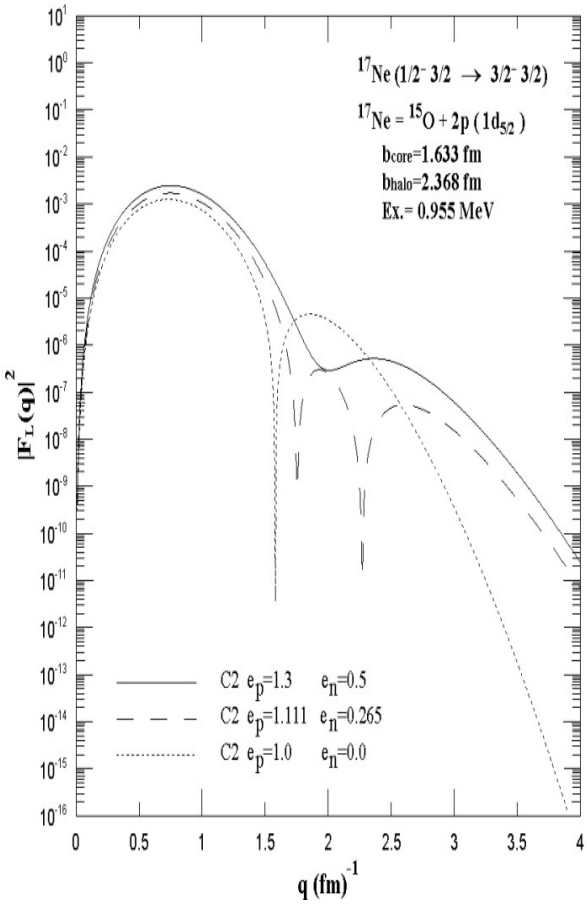

Fig. 8: The calculated inelastic longitudinal C2 form factors of ^{17}Ne with two protons in 1d$_{5/2}$ orbit and for ($J^\pi T = 3/2^- 3/2$) state.

Table 1: The calculated and experimental electric transition strengths of the excited state ($J^{\pi}T = 3/2^{-}\ 3/2$) of ^{17}Ne nucleus.

$J_i^{\pi}\ T_i$	$J_f^{\pi}\ T_f$	Configuration of ^{17}Ne nucleus	e_p	e_n	Calculated $B(C2\uparrow)$ e^2fm^4	Experimental $B(C2\uparrow)$ e^2fm^4 [33]	b_{core} (fm)	b_{halo} (fm)	Excitation energy MeV
$\frac{1}{2}^{-}\ \frac{3}{2}$	$\frac{3}{2}^{-}\ \frac{3}{2}$	^{15}O + Two protons in **sd**-Shell	1.0	0.0	105.792	66^{+18}_{-25}	1.633	2.368	2.104
			1.033	0.033	113.430				
			1.3	0.3	185.014				
			1.3	0.5	189.222				
		^{15}O + Two protons in pure $\mathbf{1d_{3/2}}$ orbit	1.0	0.0	72.579	66^{+18}_{-25}	1.606	2.640	2.260
			1.111	0.265	92.709				
			1.3	0.5	129.589				
		^{15}O + Two protons in pure $\mathbf{1d_{5/2}}$ orbit	1.0	0.0	53.520	66^{+18}_{-25}	1.633	2.368	0.955
			1.111	0.265	69.291				
			1.3	0.5	97.632				

$J^{\pi}T : 5/2^{-}\ 3/2$ state

^{17}Ne nucleus is excited here from the ground state ($J^{\pi}T = 1/2^{-}\ 3/2$) to the state ($J^{\pi}T = 5/2^{-}\ 3/2$). The experimental value of the reduced transition probability $B(C2\uparrow)$ is equal to 124(18) e^4 fm^4 [33].

The first configuration of the two halo protons of ^{17}Ne nucleus suppose that these protons are distributed over sd-shell orbits and excited with excitation energy of 2.133 MeV**.** The size parameters of the harmonic oscillator that used in the calculations are b_{core}=1.633 fm and b_{halo}=2.368 fm. Four values of the nucleon charges are employed and the *C2* Coulomb form factors that results from these values are plotted in Fig. 9 and denoted by dotted curve which is calculated by means of the bare nucleon charges (e_p=1.0 e, e_n=0.0 e), dash-dotted and dashed curves that are calculated in terms of the core polarization effective charges (e_p=1.033 e , e_n=0.033 e) and (e_p=1.3 e , e_n=0.3 e), respectively, and solid curve which reflects the use of the standard nucleon charges (e_p=1.3 e , e_n=0.5 e). The dotted curve gives only one diffraction minimum located at (q =1.34 fm^{-1}), while the others gives two diffraction minima. There is a good conformation between all curves up to $q \approx$ 2.4 fm^{-1}, and the deviation between them is appear beyond this value. The calculated transition strength $B(C2\uparrow)$ values are incompatible with the experimental value for any used nucleon charges as that shown in Table 2.

In the case of the two protons are in a pure $1d_{3/2}$ orbit (second configuration), the calculated *C2* coulomb form factors for the transition from the ground state ($J^{\pi}T = 1/2^{-}\ 3/2$) to the excited state ($J^{\pi}T = 5/2^{-}\ 3/2$) with excitation energy of 0.487 MeV are presented in Fig. 10. The size parameters are taken to be b_{core}=1.606 fm and b_{halo}=2.640 fm. Dotted curve, dashed curve and solid curves are deduced in terms of the nucleon bare charges (e_p=1.0 e , e_n=0.0 e), core polarization effective charges (e_p=1.102 e , e_n=0.255 e) and standard

nucleon charges (e_p=1.3 e, e_n=0.5 e), respectively. Dashed and solid curves gives two noticeable diffraction minima and dotted curve gives only one diffraction minimum. The experimental value of the reduced transition probability $B(C2\uparrow)$ is well described by the calculated values with bare and effective nucleon charges, as that shown in Table 2.

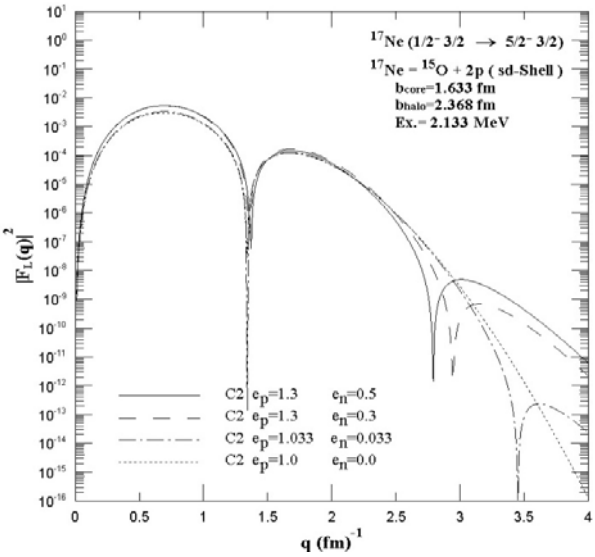

Fig. 9: The calculated inelastic longitudinal C2 form factors of ^{17}Ne with two protons in sd-shell and for ($J^{\pi}T = 5/2^{-}\ 3/2$) state.

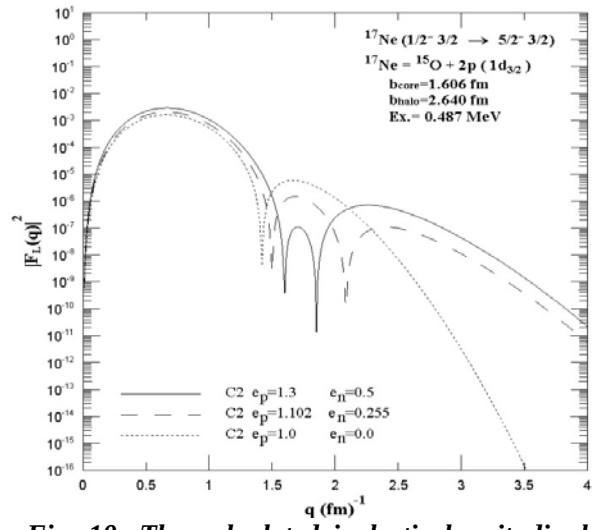

Fig. 10: The calculated inelastic longitudinal C2 form factors of ^{17}Ne with two protons in $1d_{3/2}$ orbit and for ($J^{\pi}T = 5/2^{-}\ 3/2$) state.

According to the third configuration, the two halo protons of ^{17}Ne nucleus are assumed to be in a pure $1d_{5/2}$ orbit. The calculated *C2* coulomb form factors are presented in Fig. 11 with excitation energy 0.789 MeV and size parameters b_{core}=1.633 fm and b_{halo}=2.368 fm. The Dotted, dashed and solid curves represents the calculated *C2* form factors with bare nucleon charges, core polarization effective nucleon charges (e_p=1.102 e , e_n=0.255 e) and standard nucleon charges, respectively. There is one diffraction minimum given by dotted curve and two diffraction minima given by dashed and solid curves. The theoretical and experimental values of the reduced transition probability $B(C2\uparrow)$ are given in Table 2, where the inclusion of the core polarization effective nucleon charges enhances the calculated transition strengths to get an excellent agreement with the experimental value.

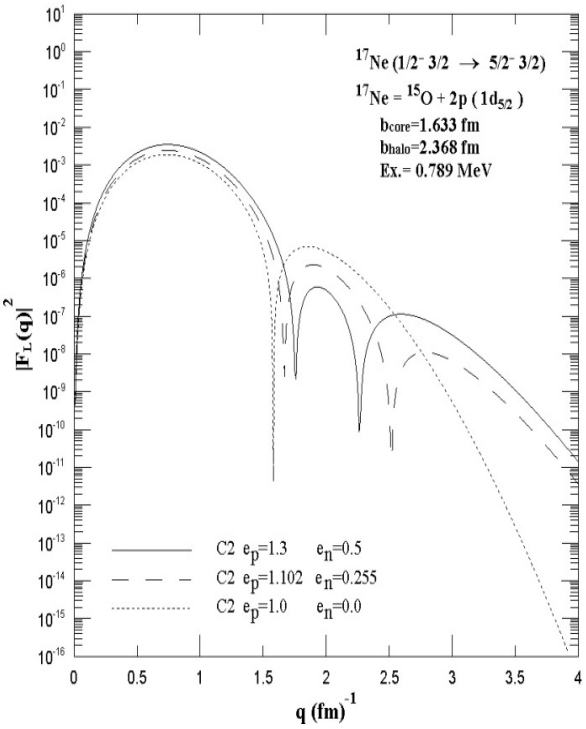

Fig. 11: The calculated inelastic longitudinal C2 form factors of ^{17}Ne with two protons in $1d_{5/2}$ orbit and for ($J^{\pi}T = 5/2^{-}\ 3/2$) state.

Table 2: The calculated and experimental electric transition strengths of the excited state ($J^{\pi}T = 5/2^{-}\ 3/2$) of ^{17}Ne nucleus.

$J_i^{\pi}\ T_i$	$J_f^{\pi}\ T_f$	Configuration of ^{17}Ne nucleus	e_p	e_n	Calculated $B(C2\uparrow)$ e^2fm^4	Experimental $B(C2\uparrow)$ e^2fm^4 [33]	b_{core} (fm)	b_{halo} (fm)	Excitation energy MeV
$\frac{1}{2}^{-}\ \frac{3}{2}$	$\frac{5}{2}^{-}\ \frac{3}{2}$	^{15}O + Two protons in **sd**-Shell	1.0	0.0	171.073	124(18)	1.633	2.368	2.133
			1.033	0.033	182.884				
			1.3	0.3	292.947				
			1.3	0.5	295.517				
		^{15}O + Two protons in pure **1d$_{3/2}$** orbit	1.0	0.0	106.875	124(18)	1.606	2.640	0.487
			1.102	0.255	132.366				
			1.3	0.5	186.599				
		^{15}O + Two protons in pure **1d$_{5/2}$** orbit	1.0	0.0	79.997	124(18)	1.633	2.368	0.789
			1.102	0.255	100.012				
			1.3	0.5	141.850				

From the previous discussions of both excited states of ^{17}Ne halo nucleus $J_f^{\pi}T_f = 3/2^{-}\ 3/2$ and $J_f^{\pi}T_f = 5/2^{-}\ 3/2$ and with the assistance of Tables 1 and 2, we can say that the sd-shell configuration of the two halo protons of ^{17}Ne nucleus fails to describe the data. In addition to the good agreement between the calculated and experimental transition strength values $B(C2\uparrow)$ when the two halo protons considered to be in a pure $1d_{3/2}$ and a pure $1d_{5/2}$, we can also say that the dominant configuration of the ^{17}Ne halo nucleus is ^{15}O core plus two protons in 1d orbit.

Conclusions

The inclusion of the two frequency shell model approach and the effective nucleon charges in the calculations that related to matter density distribution, longitudenal form factors *C0* and *C2*, and the electric transition strengths *B(C2)* for ^{17}Ne exotic nucleus lead to a markedly interpretation of the experimental results. Two different size parameters of the single particle wave functions of harmonic oscillator potential introduced in calculations and the result showed a long-density tail of the matter density distribution which is coincident with the fitted data and interpreted as evidence for the two valence protons halo in addition to the noticeable difference that is found between the calculated proton and neutron rms matter radii which also indicates that the two valence protons forming the halo. It is found that the dominant configuration of the ^{17}Ne halo nucleus is ^{15}O core plus two protons in 1d orbit.

References

[1] J. S. Vaagen, D. K. Gridnev, H. Heiberg-Andersen, B. V. Danilin, S. N. Ershov, V. I. Zagrebaev, I. J. Thompson, M. V. Zhukov and J. M. Bang, Physica Scripta, T88 (2000) 209.

[2] I. Tanihata, H. Hamagaki, O. Hashimoto, Y. Shida, N. Yoshikawa, K. Sugimoto, O. Yamakawa, T. Kobayashi and N. Takahashi, Phys. Rev. Lett. 55 (1985) 2676.

[3] I. Tanihata, H. Hamagaki, O. Hashimoto, S. Nagamiya, Y. Shida, N. Yoshikawa, O. Yamakawa, K. Sugimoto, T. Kobayashi, D.E. Greiner, N. Takahashi and Y. Nojiri, Phys. Lett. B 160 (1985) 380.
[4] P.G. Hansen and B. Jonson, Europhys. News, 4 (1987) 409.
[5] T. Kobayashi, O. Yamakawa, K. Omata, K. Sugimoto, T. Shimoda, N. Takahashi and I. Tanihata, Phys. Rev. Lett. 60 (1988) 2599.
[6] N. Fukuda1, T. Nakamura, N. Aoi, N. Imai, M. Ishihara, T. Kobayashi, H. Iwasaki, T. Kubo, A. Mengoni, M. Notani, H. Otsu, H. Sakurai, S. Shimoura, T. Teranishi, Y. X. Watanabe and K. Yoneda, Phys. Rev. C 70 (2004) 054606.
[7] T. Aumann, D. Aleksandrov, L. Axelsson, T. Baumann, M. J. G. Borge, L. V. Chulkov, J. Cub, W. Dostal, B. Eberlein, Th. W. Elze, H. Emling, H. Geissel, V. Z. Goldberg, M. Golovkov, A. Grünschloß, M. Hellström, K. Hencken, J. Holeczek, R. Holzmann, B. Jonson, A. A. Korshenninikov, J. V. Kratz, G. Kraus, R. Kulessa, Y. Leifels, A. Leistenschneider, T. Leth, I. Mukha, G. Münzenberg, F. Nickel, T. Nilsson, G. Nyman, B. Petersen, M. Pfützner, A. Richter, K. Riisager, C. Scheidenberger, G. Schrieder, W. Schwab, H. Simon, M. H. Smedberg, M. Steiner, J. Stroth, A. Surowiec, T. Suzuki, O. Tengblad M. V. Zhukov, Phys. Rev. C59 (1999) 1252.
[8] T. Nakamura, A. M. Vinodkumar, T. Sugimoto, N. Aoi, H. Baba, D. Bazin, N. Fukuda, T. Gomi, H. Hasegawa, N. Imai, M. Ishihara, T. Kobayashi, Y. Kondo, T. Kubo, M. Miura, T. Motobayashi, H. Otsu, A. Saito, H. Sakurai, S. Shimoura, K. Watanabe, Y. X. Watanabe, T. Yakushiji, Y. Yanagisawa, and K. Yoneda, Phys. Rev. Lett. 96 (2006) 252502.
[9] G.F. Bertsch and H. Esbensen, Ann. Phys. 209 (1991) 327.
[10] M.V. Zhukov, B.V. Danilin, D.V. Fedorov, J.M. Bang,I.J. Thompson and J.S. Vaagen, Phys. Rep. 231 (1993) 151.
[11] A. Ozawa, T. Suzuki and I. Tanihata, Nucl. Phys. A 693 (2001) 32.
[12] J. Al-Khalili, Lect. Notes Phys. 651(2004)77
[13] T. T. S. Kuo, H. Muether and K. Amir-Azimi-Nili, Nucl. Phys. A606 (1996) 15.
[14] T. T. S. Kuo, F. Krmpotic and Y. Tzeng, Phys. Rev. Lett. 78 (1997) 2708.
[15] T. Deforest, Jr. and J. D. Walecka, Adv. Phys. 15 (1966) 1.
[16] B. A. Brown, R. Radhi and B. H. Wildenthal, Phys. Rep. 101 (1983) 313.
[17] P. J. Brussaard and P. W. M. Glaudemans "Shell Model Applications In Nuclear Spectroscopy" Amsterdam: North Holand (1977).
[18] G. Berstch, J. Borysowicz and H. McManus, W. G. Love, Nucl. Phys. A 284 (1977) 399.
[19] I. Talmi, Helv. Phys. Acta 25(1952) 185.
[20] M. Moshinsky, Nucl. Phys. 13 (1959) 104.
[21] T. W. Donnely and I. Sick, Rev. Mod. Phys. 56 (1984) 461.
[22] J. P. Glickman, W. Bertozzi, T. N. Buti, S. Dixit, F. W. Hersman, C. E. Hyde-Wright, M. V. Hynes, R. W. Lourie, B. E. Norum J. J. Kelly, B. L. Herman and D. J. Millener, Phys. Rev. C 43 (1990) 1740.
[23] B. A. Brown, B.H. Wildenthal, C.F. Williamson, F.N. Rad, S. Kowalski, H. Crannell and J.T. O'Brien, Phys. Rev. C 32 (1985) 1127.
[24] I. S. Towner "A shell model description of light nuclei" Clarendon press, Oxford (1971).
[25] M. V. Zhukov and I.J. Thompson, Phys. Rev. C52 (1995) 3505.
[26] A. S. Jensen, K. Riisager, D.V. Federov and E. Garrido, Rev. Mod. Phys. 76 (2004) 215.

[27]Richard B. Firestone. The Berkeley Laboratory Isotopes Project's, Exploring the Table of Isotopes, May 22, 2000. http://ie.lbl.gov/education/isotopes.htm
[28] B. A. Brown, A. Etchegoyen, N. S. Godwin, W. D. M. Rae, W. A. Richter, W. E.Ormand, E. K. Warburton, J. S. Winfield, L. Zhao and C. H. Zimmerman, Oxbash for windows, MSU- NSCL report number 1289 (2005).
[29] D. J. Millener and D. Kurath, Nucl. Phys. A255 (1975) 315
[30] K. Tanaka, M. Fukuda, M. Mihara, M. Takechi, D. Nishimura, T. Chinda, T. Sumikama, S. Kudo, K. Matsuta, T. Minamisono, T. Suzuki, T. Ohtsubo, T. Izumikawa, S. Momota, T. Yamaguchi, T. Onishi, A. Ozawa, I. Tanihata and T. Zheng, Phys. Rev. C82 (2010) 044309-1.
[31] Y. Horikawa, Prog. Theor. Phys. 47, 867 (1972).
[32] E. A. Knight, R. P. Singhal, R. G. Arthur, and M. W. S. Macauley, J. Phys. G7 (1981) 1115.
[33] M. J. Chromik, P. G. Thirolf, M. Thoennessen, B. A. Brown, T. Davinson, D. Gassmann, P. Heckman, J. Prisciandaro, P. Reiter, E. Tryggestad and P. J. Woods, Phys. Rev. C 66 (2002) 024313.